processes

MDPI

Article

Influence of Hydrophilic Groups of Surfactants on Their Adsorption States and Wetting Effect on Coal Dust

Chaohang Xu [1], Tongyuan Zhang [1], Sijing Wang [1], Jian Gan [2,3,4] and Hetang Wang [2,3,*]

[1] School of Safety Science and Emergency Management, Wuhan University of Technology, Wuhan 430070, China; xchwhut@whut.edu.cn (C.X.); zhangtongyuan54@163.com (T.Z.); mroirr@163.com (S.W.)
[2] Key Laboratory of Gas and Fire Control for Coal Mines (China University of Mining and Technology), Ministry of Education, Xuzhou 221116, China; 18663287873@126.com
[3] State Key Laboratory of Coal Mine Disaster Prevention and Control (China University of Mining and Technology), Xuzhou 221116, China
[4] School of Safety Science and Engineering, Anhui University of Science and Technology, Huainan 232001, China
* Correspondence: wanghetang@cumt.edu.cn

Abstract: Surfactants are often used in the process of coal dust suppression, and the wetting effect is greatly affected by the surfactant hydrophilic group structures. In order to explore the influence of hydrophilic groups of surfactants on their adsorption states and wetting effect on coal dust, three surfactants with similar hydrophilic groups were selected, namely, anionic surfactant sodium dodecyl sulfate (SDS), anionic-nonionic surfactant alkyl ether sulfate (AES), and nonionic surfactant alkyl polyoxyethylene ether-3 (AEO-3). To assess surfactant efficiency, surface tension, wetting time, infrared spectra, and wetting heat were analyzed. These parameters provide insights into molecular adsorption, interfacial behavior, and energy changes during wetting. The different adsorption states of surfactants on the coal dust surface due to EO and SO_4^{2-} hydrophilic groups were analyzed. Results show that both anionic surfactant SDS and nonionic surfactant AEO-3 form the monolayer adsorption structure on the coal dust surface. Due to the electrostatic repulsion of SO_4^{2-} groups, the adsorption density of SDS is lower than that of AEO-3, which results in the higher wetting heat of AEO-3 compared to SDS. In addition, the EO groups without electrostatic repulsion make AEO-3 molecules more tightly adsorbed at the air–liquid interface, causing the minimal surface tension. Therefore, the wetting time of AEO-3 is shorter than that of SDS. The anionic-nonionic surfactant AES has both EO and SO_4^{2-} groups. Because the EO groups in the inner surfactant adsorption layer can attract Na^+ ions to distribute around them, the free AES molecules further form the outer adsorption layer under the electrostatic attraction between SO_4^{2-} groups and Na^+ ions. The double-layer adsorption structure causes the hydrophobic groups of the outer AES molecules to face outward, the hydrophobic sites on the coal dust surface are not completely transformed into hydrophilic sites. Although AES exhibits the highest adsorption density, it has the lowest wetting heat and the longest wetting time. The research results can provide theoretical guidance for the selection of suitable surfactants for coal dust suppression.

Keywords: surfactants; coal dust; adsorption state; wetting time; wetting heat

check for updates

Academic Editors: Haiping Zhang, Hui Zhang and Hsin Chu

Received: 19 March 2025
Revised: 28 April 2025
Accepted: 19 May 2025
Published: 21 May 2025

Citation: Xu, C.; Zhang, T.; Wang, S.; Gan, J.; Wang, H. Influence of Hydrophilic Groups of Surfactants on Their Adsorption States and Wetting Effect on Coal Dust. *Processes* **2025**, *13*, 1612. https://doi.org/10.3390/pr13051612

Copyright: © 2025 by the authors. Licensee MDPI, Basel, Switzerland. This article is an open access article distributed under the terms and conditions of the Creative Commons Attribution (CC BY) license (https://creativecommons.org/licenses/by/4.0/).

1. Introduction

Coal is one of the most important sources of energy in the world, and according to the 2023 BP Statistical Yearbook of World Energy, global coal production increased by 7.9%

in 2022 compared to 2021, accounting for the second largest share of the world's primary energy consumption [1–3]. The mining process of coal is often accompanied by a variety of disasters, such as gas explosions, coal dust explosions, lung diseases, spontaneous combustion of coal, and so on. Various mine disasters will change or dissipate with the different geological conditions, but the disaster of coal dust always accompanies the process of mining work, which is a nightmare that no coal mine can avoid [4–7].

A variety of dust removal techniques have been used so far, including water spraying, chemical dust suppression, water injection into coal seams, and ventilation [8–13]. Among them, spray dust reduction, chemical dust suppression, and coal bed water injection are all means of dust control that use water as the main medium, which shows that water-based materials are important for coal dust management. Most coals have low energy surfaces, while pure water has high surface tension, which leads to a poor wetting effect of pure water on coal dust. Surfactants can be used to reduce the water surface tension and improve the wetting ability of the solution for coal dust, and are often used as wetting agents in the field of coal dust suppression. Therefore, a large number of scholars have tried to enhance the wetting effect of coal dust by adding surfactants to water, thus improving the dust suppression effect [14–17].

According to the hydrophilic group structures, surfactants can be categorized into anionic, cationic, nonionic, and amphoteric types, and each type of surfactant consists of many different hydrophilic head groups and hydrophobic tail groups. The complexity of surfactant structures makes it difficult to select a surfactant that can quickly wet a specific coal dust based on a generalized approach. The only way to do so is to try potential surfactants, which is not only a huge amount of work, but also has a great deal of blindness [18–21]. Thus, the study of the effect of surfactant hydrophilic group structure on the coal dust wetting ability has a huge role in the subsequent targeted and rapid selection of specific surfactants to inhibit specific coal dust [22–24].

The adsorption states and wetting ability of different surfactants on the coal dust are the research focus in the field of coal dust deposition. Crawford et al. [25] investigated the ability of three surfactants (anionic, cationic, and nonionic surfactants) to change the surface hydrophobicity of three Australian coals, and the results showed that different grades of coals and surfactants with different properties had a significant effect on the surface wettability of coals. Xu et al. [26] studied the effect of anionic surfactants with different structures on the wettability of coal dust, and the results revealed that surface tension, adsorption density, and hydrophilic–lipophilic balance (HLB) values had different degrees of influence on the wetting time of coal dust. Liu et al. [27] found that the adsorption capacity of cationic gemini surfactants on the surface of lignite was significantly higher than that of ordinary cationic and anionic surfactants, which was due to the strong electrostatic attraction between the surfactants and lignite. As a result, the hydrophobicity of lignite increased and the wettability decreased after the adsorption of cationic gemini surfactants. Wang et al. [28] tested the wetting ability of surfactants on coal dust based on the physicochemical properties of different coal samples. It was found that anionic surfactants had stronger wetting ability compared with nonionic surfactants, but the same anionic surfactants had different wetting abilities on coal dust with different degrees of metamorphism. However, the effect of different types and molecular structures of surfactants on the wettability of coal dust surface has not been analyzed, which is a very valuable and promising direction for further research.

In this work, three types of surfactants with similar hydrophilic groups, i.e., sodium dodecyl sulfate (SDS), alkyl ether sulfate (AES), and alkyl polyoxyethylene ether-3 (AEO-3) were chosen. The hydrophilic part of the anionic surfactant SDS is one SO_4^{2-} group. The hydrophilic part of the nonionic surfactant AEO-3 is three EO groups. The hydrophilic part of

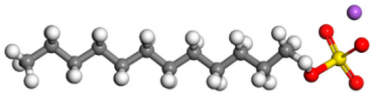
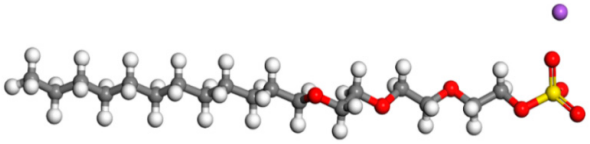
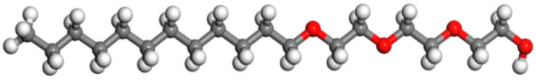
AES is one SO_4^{2-} group and three EO groups, which can be considered an anionic-nonionic surfactant. By skillfully selecting the above three surfactants, the different adsorption states and wetting effects caused by the difference in the hydrophilic group structures of surfactants can be deeply analyzed. This research is helpful to reveal the micro-mechanism of the hydrophilic group structures of surfactants on the improvement of coal dust wettability.

2. Materials and Methods

2.1. Materials

The surfactants used in the experiments were sodium dodecyl sulfate (SDS, purity ≥ 99%, Qingdao Yousuo Chemical Technology Co., Qingdao, China), alkyl ether sulfate (AES, purity ≥ 99%, Qingdao Yousuo Chemical Technology Co., Qingdao, China), and alkyl polyoxyethylene ether-3 (AEO-3, purity ≥ 99%, Qingdao Yousuo Chemical Technology Co., Qingdao, China). Material Studio 7.0 (Accelrys, San Diego, CA, USA) was used for molecular structure modeling. A comparison of the type and molecular structure of each surfactant is shown in Table 1. The difference in the three surfactant molecules is mainly their hydrophilic groups, as mentioned above. By skillfully selecting these three surfactants, the influence of the difference in surfactant hydrophilic group structure on the wetting effect of coal dust can be explored. Distilled water was used in all experiments.

Table 1. Surfactant type and molecular structure.

Surfactant	Type	Molecular Structure
SDS	Anionic	
AES	Anionic-nonionic	
AEO-3	Nonionic	

Note: —O atoms; —S atoms; —Na atoms; —C atoms; —H atoms.

2.2. Preparation of Surfactant Solution

The concentrations of SDS, AES, and AEO-3 solutions were all prepared at 0.005 wt%, 0.05 wt%, 0.1 wt%, 0.2 wt%, and 0.3 wt%. All solutions were stirred at 35 °C for 1 h using a thermostatic magnetic stirrer to completely dissolve the solutes, and then each solution was left to stand for 24 h to allow the generated foam on the solution surface to completely disappear.

2.3. Surface Tension Measurement

The surface tension of all solutions was measured using a JYW-200B surface tension meter with the platinum ring method. Before each measurement, the remaining solution on the platinum ring was rinsed with pure water and dried with an alcohol lamp. Each solution was measured more than five times. The three sets of data with an error of less than 1% were selected and averaged to obtain the surface tension. All tests were kept at 25 °C.

2.4. Wetting Time Measurement

A gas-fertilized coal sample from Shandong Hongqi Coal Mine was selected for the wetting experiments, with a particle size of 200–300 mesh after treatment in the mill.

Proximate analysis revealed that the coal sample contained 1.21 wt% moisture, 19.32 wt% ash, 31.49 wt% volatile, and 47.98 wt% fixed carbon. A total of 50 mL of surfactant solution was added into a beaker, and 0.2 g of coal dust was weighed and quickly poured onto the surface of the solution. The time required for all the coal dust to completely settle below the liquid surface was monitored and recorded. This recorded time is defined as the wetting time [10,13]. The wetting ability of different solutions was compared using the wetting time. The wetting time measurement experiment was conducted three times under the same conditions, and the average value was taken.

2.5. Infrared Spectrum Measurement

The infrared spectra of raw and surfactant-wetted coal samples were tested by a Nicolet Model 6700 Fourier Transform Infrared Spectrometer (FTIR). Prior to testing, background spectra were obtained using pure potassium bromide powder. The raw coal sample was then placed in a diffuse reflectance cuvette and the surface was scraped and pressed. The test was performed in the wave number range of 650–4000 cm^{-1} with a resolution of 4 cm^{-1} and 64 scans. The coal samples wetted by surfactant solution were filtered through filter paper and were then put into a vacuum drying oven and dried at 60 °C for 24 h. After cooling, the infrared spectra of surfactant-wetted coal samples were tested according to the above steps.

2.6. Wetting Heat Measurement

A Setaram C80 calorimeter was used to determine the wetting heat H (J/g) released during the contact process of the coal sample with the solution. A membrane mixing cell was selected for membrane separation of the two components. A measure of 0.1 g of sample was placed into the bottom of the membrane mixing cell and the membrane mixing cell divide was divided the into upper and lower layers with a piece of tin foil. Two milliliters of surfactant solution were injected into the upper layer of the mixing cell. The mixing cell assembly was then placed into the adiabatic chamber of the microcalorimeter. Once the system stabilized, the tin foil diaphragm was pierced to initiate mixing of the solid and liquid phases. No solid material was added to the lower layer of the reference cell, and all operations were performed in the same manner as in the sample cell. The heat flow curve was recorded and integrated manually to obtain the wetting heat value.

3. Results and Discussion

3.1. Surface Tension

An important factor affecting the wetting effect of coal dust is the surface tension of the liquid, and the main reason for the poor wetting ability of pure water on coal dust is its high surface tension. Surfactants can effectively reduce the surface tension of the solution, thus weakening the energy barrier when coal dust particles enter the solution and improving the dust trapping efficiency [29].

The surface tension curves of SDS, AES, and AEO-3 solutions are shown in Figure 1. The surface tension of each surfactant decreases substantially when the solution mass fraction is increased from 0 to 0.005%, showing different trends as the subsequent concentration continues to increase. Both AES and SDS solutions show a large fluctuation trend. The lowest point of surface tension of AES solution is located in the mass concentration of 0.05%, which is the critical micelle concentration of AES, and the surface tension is 29.59 mN/m. With the increase in AES concentration, the surface tension slightly increases, and ultimately stabilizes at about 35 mN/m. As the concentration increases, the surface tension of SDS solution continues to decrease. When the concentration reaches 0.1%, which is the critical micelle concentration of SDS, the surface tension comes to the lowest point of 29.32 mN/m

and ultimately stabilizes at about 32 mN/m. Compared with AES and SDS, the fluctuation of AEO-3 surface tension is extremely small. The critical micelle concentration of AEO-3 is 0.005%. When the concentration of AEO-3 is higher than 0.005%, the surface tension does not change much, stabilizing at a smooth state of about 25 mN/m. This shows that the addition of AEO-3 can greatly reduce the surface tension of pure water.

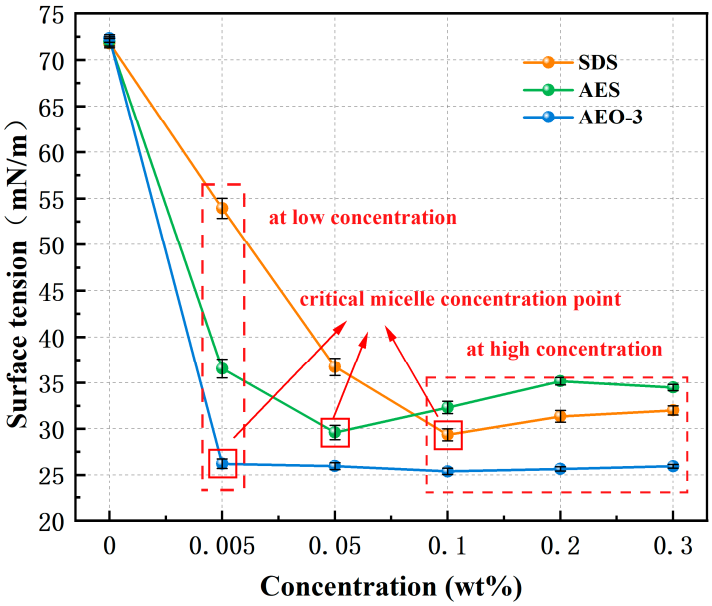


Figure 1. Surface tension of SDS, AES, and AEO-3 solutions.

When the surfactant concentration is higher than 0.1%, the effectiveness in reducing the surface tension is ranked as AEO-3 > SDS > AES, which is related to the adsorption states of surfactant molecules at the air–water interface, as shown in Figure 2. AES and SDS both exhibit negative charges after ionization in water. However, AES imports EO groups, which leads to the enhanced hydrophilicity. As the surfactant concentration increases, AES solution reaches the critical micelle concentration faster than SDS, and the number of micelle aggregates is also higher. In addition, when SDS and AES reach a saturated adsorption state at the air–water interface, the occupied interface area of each surfactant molecule of AES and SDS is 52 $Å^2$ and 42.44 $Å^2$, respectively [30,31]. Therefore, the number of SDS molecules adsorbed at the air–water interface is more than that of AES molecules, resulting in the lower surface tension of SDS than that of AES. Compared with SDS and AES surfactants, AEO-3 has no electrostatic repulsion. At the same concentration, AEO-3 surfactant molecules are more easily enriched in the adsorption layer formed at the air–water interface, as shown in Figure 2c, so the surface tension of AEO-3 solution is the lowest.

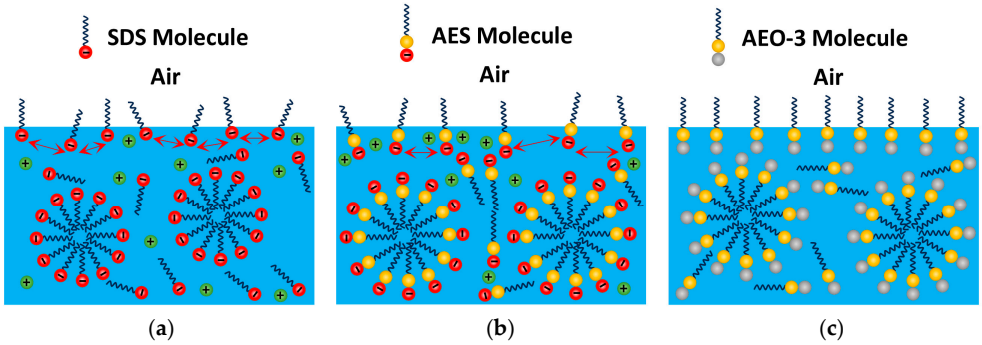


Figure 2. Schematic illustration of the air–water interface adsorption state of surfactant molecules: (**a**) SDS, (**b**) AES, (**c**) AEO-3.

3.2. Wetting Time of Coal Dust

The time for different surfactant solutions to wet the coal dust is shown in Table 2 and Figure 3. When the surfactant concentration is lower than 0.005%, the wetting time is extremely long or more than 24 h, which indicates that the coal dust is wetted for a long time or cannot be wetted. When the concentration of surfactant is more than 0.05%, the wetting time gradually decreases with the increase in surfactant concentration.

Table 2. Wetting time of coal dust in three surfactant solutions.

Surfactant Concentration	Coal Dust Wetting Time		
	SDS	AES	AEO-3
0%	>24 h	>24 h	>24 h
0.005%	>24 h	>24 h	11,124.44 s
0.05%	1703.90 s	1915.96 s	776.15 s
0.1%	1096.59 s	1344.72 s	176.71 s
0.2%	269.16 s	705.78 s	266.30 s
0.3%	207.31 s	326.82 s	163.24 s

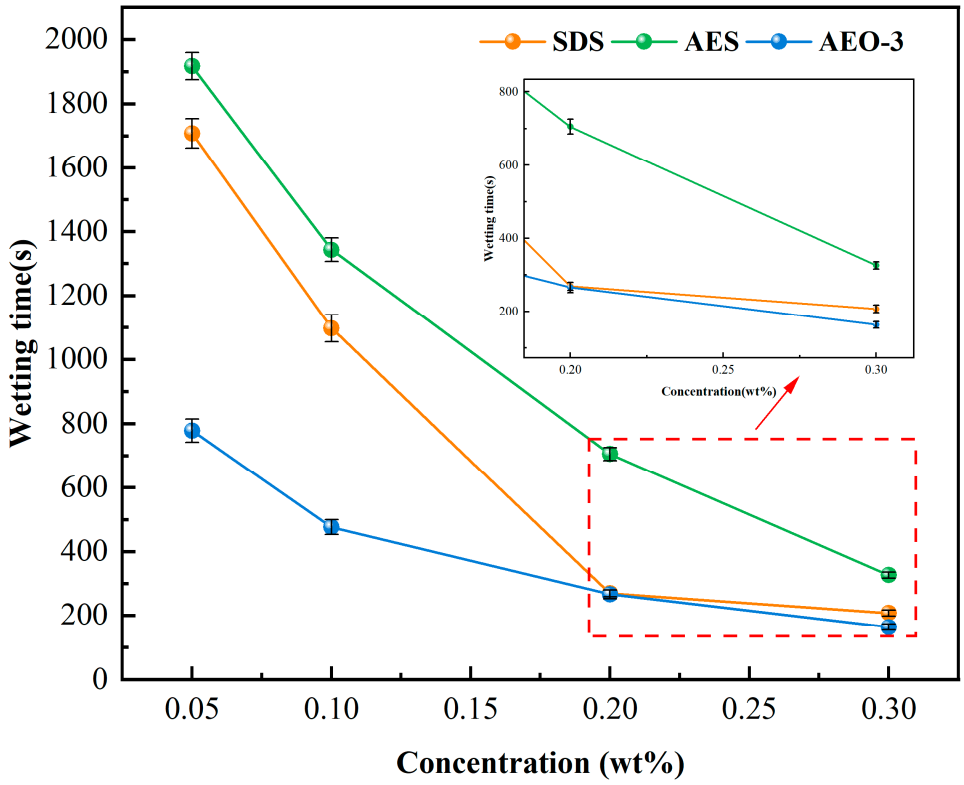


Figure 3. Wetting time curves of coal dust in three surfactant solutions.

The relationship between the solution surface tension and the wetting time is analyzed as follows. When the surfactant concentration is lower than 0.05%, the solution surface tension decreases with the increase in surfactant concentration. Therefore, the time for coal dust to settle below the surface has been significantly shortened in all the different solutions. This indicates that the decrease in surface tension can reduce the energy barrier of coal dust into the surfactant solution and improve the wetting effect. When the surfactant concentration exceeds 0.1%, the surface tension becomes stable. But, the wetting time continues to decrease with the surfactant concentration increase, which indicates that the surface tension has little effect on the solution's ability to wet coal dust. At this time, the adsorption of surfactants on the coal dust surface begins to play a role. There are many hydrophobic

groups on the surface of coal dust, which manifest as hydrophobic sites, leading to the hydrophobicity of coal dust. As the concentration of surfactant solution increases, more hydrophobic sites on the surface of coal dust bind to the surfactant hydrophobic groups, leading to the surfactant hydrophilic groups towards outward. It makes the hydrophobic points on the coal dust surface become hydrophilic points, improving the hydrophilicity of coal dust and shortening the wetting time. In addition, the order of wetting time of the three surfactants is AEO-3 < SDS < AES at the surfactant concentration greater than 0.1%. This is also related to the different adsorption state of surfactants on the coal dust surface, which will be explained in the following text.

3.3. Adsorption State

Studies in the literature have shown that by comparing the infrared spectra of mineral particles before and after the adsorption of surfactants, the adsorption state of surfactants on the surface of mineral particles can be analyzed [27,32–34]. So, this method is also used in this work to study the adsorption state of surfactants on the surface of coal dust, and then the reason for the difference in the hydrophilic group structures of the surfactants on the wetting effect of coal dust is explored.

Firstly, the characteristic transmittance peak of the surfactants must be determined. Due to the presence of EO groups in both AEO-3 and AES molecules, EO groups were selected to characterize the adsorbed AEO-3 and AES surfactants on the coal dust surface. The wave number of EO groups in the infrared spectrum is 913 cm^{-1} [35]. For AES and SDS surfactants, SO_4^{2-} was selected as the characteristic absorption group, corresponding to a wave number of 1114 cm^{-1} in the infrared spectrum [36,37]. Due to the absence of benzene rings in all three surfactants, benzene rings were selected as the characteristic absorption peak of the raw coal sample, and the wave number of the C-H bond's absorption peak of benzene rings is 3040 cm^{-1} [38].

The infrared spectra of the raw coal sample are shown in Figure 4, and the transmittance peaks of EO groups, SO_4^{2-} groups, and C-H bond of the benzene ring can also be observed at 913 cm^{-1}, 1114 cm^{-1}, and 3040 cm^{-1} respectively. If the surfactants are adsorbed on the coal dust surface, the peak intensities of the transmittance peaks at 913 cm^{-1} and 1114 cm^{-1} would be higher than those of the raw coal sample. The flatness of the coal dust surface in the sample cell can easily affect the absolute intensity of the transmittance peak. In order to more accurately reflect the adsorption of surfactant on the surface of the coal dust, the absolute intensity of the transmittance peaks at 913 cm^{-1} and 1114 cm^{-1} are not used for comparison [26]. The ratio of the transmittance peak intensities at 913 cm^{-1} and 1114 cm^{-1} to the transmittance peak intensity at 3040 cm^{-1} is used as an index to compare the difference in the adsorption states of surfactants on the coal dust surface. The smaller the ratio exhibits, the higher the adsorption density of the surfactant on the coal dust surface will exhibit.

Coal samples wetted by surfactant solutions at concentrations of 0.005%, 0.1%, and 0.3% were selected. The FTIR spectra of the surfactant-wetted coal samples are shown in Figures 5–7. Table 3 shows the transmittance of EO groups and benzene ring C-H bonds and their ratios of coal samples treated with AEO-3 and AES. The transmittance of SO_4^{2-} groups and benzene ring C-H bonds and their ratios of coal samples treated with AES and SDS are listed in Table 4. In Figure 4, the transmittance of the EO groups, SO_4^{2-} groups and benzene ring C-H bonds of the raw coal sample are 79.17384, 69.33411, and 87.97184, respectively. After calculation, the ratio of the transmittance of the EO groups to the benzene ring C-H bonds is 0.89999072, and the ratio of the transmittance of the SO_4^{2-} groups to the benzene ring C-H bonds is 0.78813982. From Tables 3 and 4, it can be seen that the two ratios of the coal samples wetted by the three surfactants are lower than that

of the raw coal sample, which indicates that the surfactants have adsorbed on the coal dust surface.

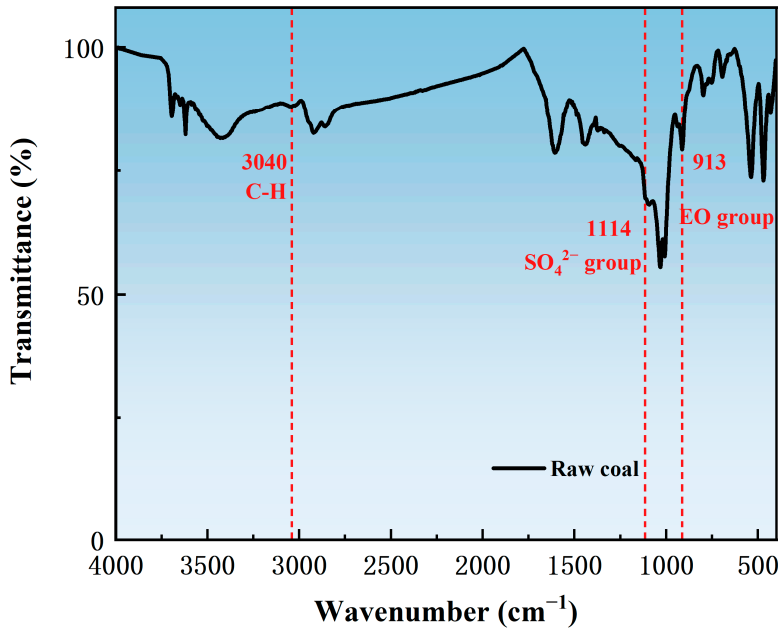


Figure 4. Infrared characteristic peaks of raw coal sample.

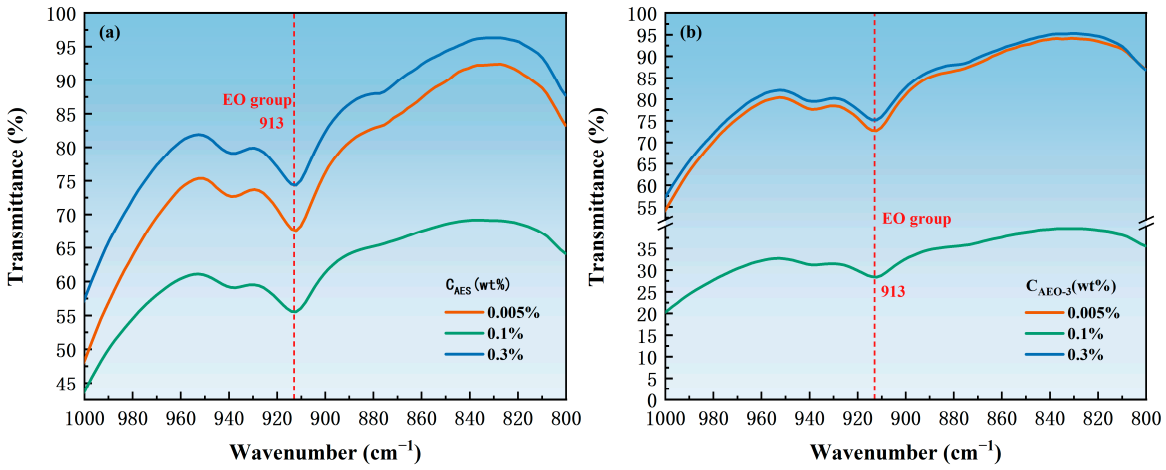


Figure 5. Infrared characteristic peaks of EO groups: (**a**) AES; (**b**) AEO-3.

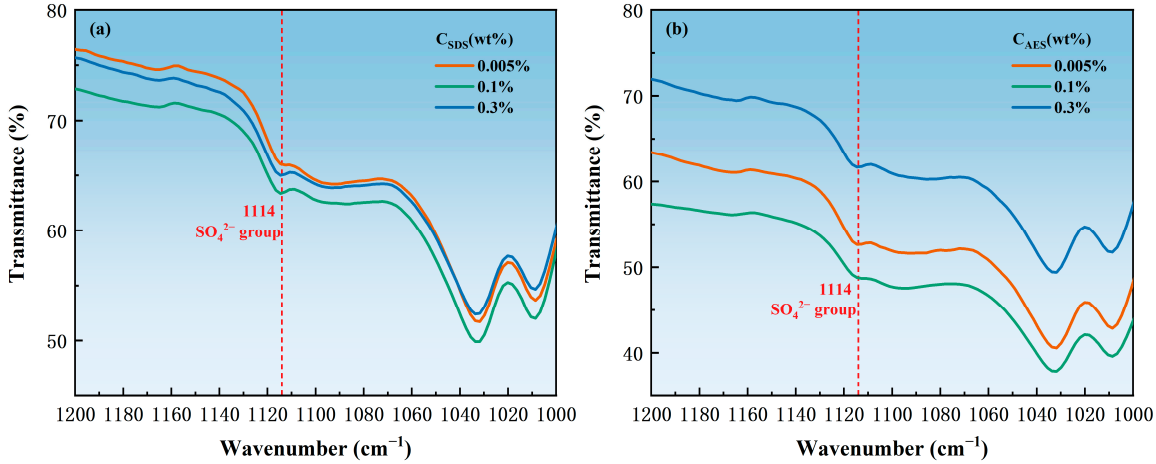


Figure 6. Infrared characteristic peaks of SO_4^{2-} groups: (**a**) SDS; (**b**) AES.

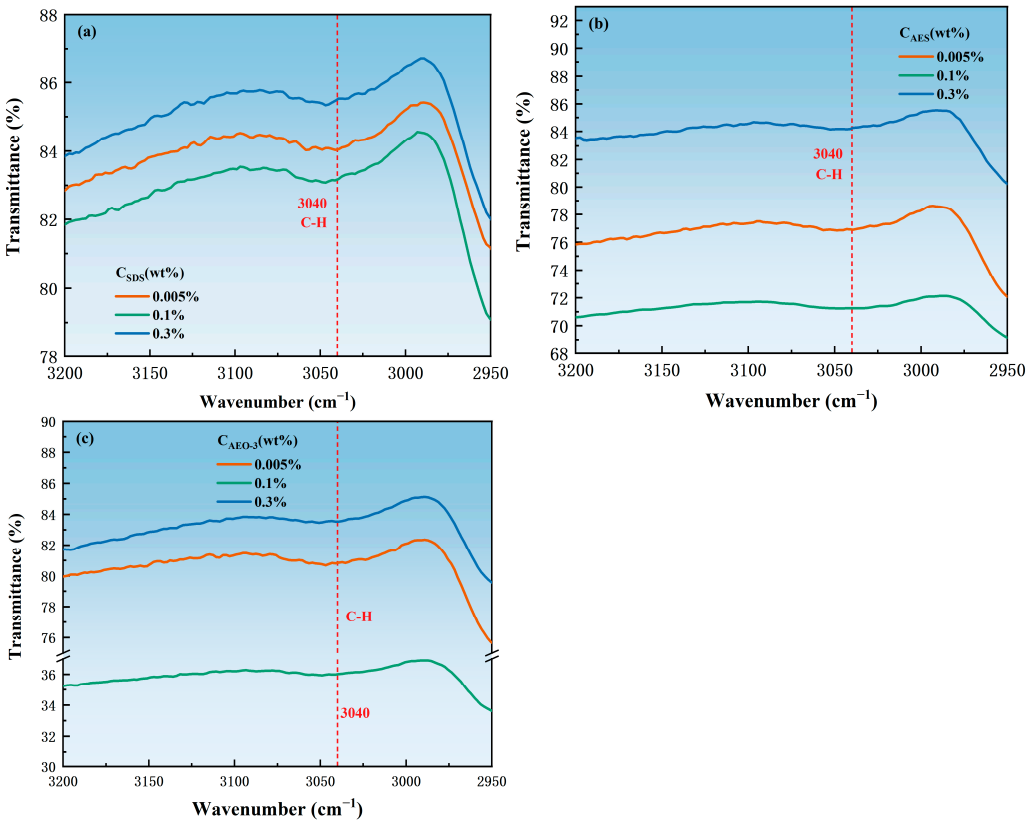


Figure 7. Infrared characteristic peaks of benzene ring C-H bonds: (**a**) SDS; (**b**) AES; (**c**) AEO-3.

Table 3. Transmittance of EO groups and benzene ring C-H bonds and their ratios of coal samples treated with AEO-3 and AES solutions.

Surfactant	Concentration (wt.%)	EO Groups	Benzene Ring C-H Bond	Ratio of the Transmittance of the EO Groups to the C-H Bond of the Benzene Ring
AEO-3	0.005	72.69923	80.84245	0.89974
	0.1	28.39412	36.02352	0.78821
	0.3	75.18254	83.56574	0.89968
AES	0.005	67.59277	76.89948	0.87898
	0.1	55.54300	71.25000	0.77955
	0.3	74.36169	84.27282	0.88239

Table 4. Transmittance of SO_4^{2-} groups and benzene ring C-H bonds and their ratios of coal samples treated with AES and SDS solutions.

Surfactant	Concentration (wt.%)	SO_4^{2-} Groups	Benzene Ring C-H Bond	Ratio of the Transmittance of the SO_4^{2-} Groups to the C-H Bond of the Benzene Ring
AES	0.005	52.63848	76.89948	0.68451
	0.1	48.75639	71.25000	0.68430
	0.3	61.68929	84.27282	0.73202
SDS	0.005	66.03024	84.04665	0.78564
	0.1	63.36406	83.18496	0.76172
	0.3	65.16047	85.38580	0.76313

For the same surfactant, the ratios show a tendency of decreasing and then increasing with the concentration increase. This indicates that the surfactant adsorption density on the coal dust surface increases first and then decreases gradually. At low concentration, the

number of free surfactant molecules in the solution is very small, which leads to the low adsorption density of surfactant on the coal dust surface. With the increase in surfactant concentration, there are many free surfactant molecules, which causes a large number of surfactants to be adsorbed on the surface of coal sample. As the surfactant concentration continues to increase, a large number of micelles are formed in the surfactant solution. At this point, each micelle has an adsorption effect on free surfactant molecules. The hydrophobic sites on the coal dust surface also have adsorption effects on free surfactant molecules. Therefore, there is a competitive adsorption between micelles and coal dust, which results in the reduction in the surfactant adsorption density on the coal dust surface.

In addition, comparing the ratio values of the three surfactant-treated coal samples with the ratio values of the raw coal sample in a comprehensive manner, it can be concluded that the adsorption density is ranked as AES > AEO-3 > SDS, which is related to the difference in surfactant hydrophilic group structures. The explanation is as follows. As shown in Figure 8a, the negative charge carried by the SO_4^{2-} groups leads to a high electrostatic repulsion between neighboring SDS molecules, which increases the spacing between neighboring surfactant molecules. Thus, the adsorption density of SDS is the lowest. As for AES, studies have shown that the EO groups can attract Na^+ ions to distribute around it [39,40]. The negatively charged AES molecules that have been ionized combine with the Na^+ ions attracted by the EO groups. On the one hand, it leads to a weakening of the electrostatic repulsion between adjacent surfactant molecules. On the other hand, it leads to the formation of a double-layer adsorption structure of the AES molecules on the surface of the coal dust, as shown in Figure 8b. Therefore, the adsorption density of AES molecules among the surfactants adsorbed with coal dust appears as the highest. Due to the double-layer adsorption, the surfactant hydrophobic groups still face outward. The hydrophobic sites of coal dust treated with AES are not changed to hydrophilic sites. So, even though AES has the highest adsorption density among them, its wetting time is still the longest. As shown in Figure 8c, for nonionic surfactant AEO-3, there is no electrostatic repulsion between molecules. Therefore, the adsorption density of AEO-3 on coal dust surface is higher than SDS. In addition, due to the absence of Na^+ ions, the presence of EO groups does not lead to the formation of double-layer adsorption structure like AES, which resulted in a lower adsorption density on the coal dust surface than AES.

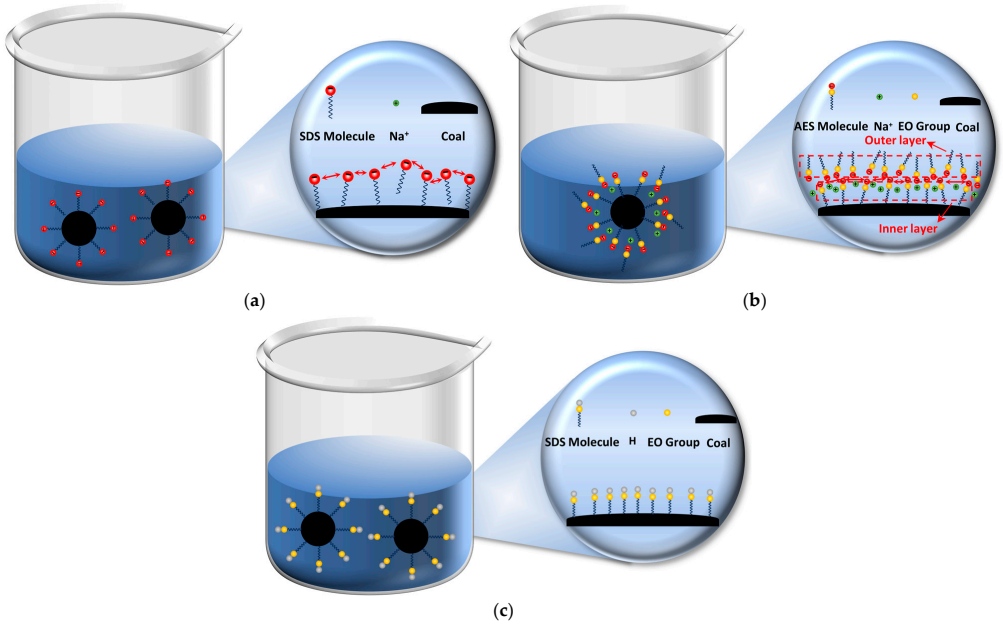


Figure 8. Schematic illustration of the three surfactants' adsorption states on the coal dust surface: (**a**) SDS; (**b**) AES; (**c**) AEO-3.

3.4. Wetting Heat

3.4.1. Wetting Heat Flow Curve of Pure Water

The wetting process of water on the coal dust is the process of air being replaced by liquid on the coal sample surface, which means the interaction between water molecules and the coal sample surface is stronger than the hydrogen bonding between water molecules [41]. This is a spontaneous process, which means that the wetting process is the process of Gibbs free energy decrease, i.e., $\Delta G < 0$. Water molecules are wetted from the liquid state to the solid surface, and the water molecules at the coal–water interface change from three-dimensional spatial motion to two-dimensional planar motion. The molecular degrees of freedom decrease. So, the adsorption process is an entropy decreasing process, i.e., $\Delta S < 0$. According to the thermodynamic equation $\Delta G = \Delta H - T\Delta S$, so the ΔH of the wetting process should be negative, i.e., $\Delta H < 0$. The thermodynamic theory analysis results indicate that the wetting process of water on coal is a spontaneous exothermic process [27].

Figure 9 shows the wetting heat flow curves between pure water and the coal sample in the first 25 min (at a constant temperature of 30 °C). When pure water comes into contact with dry coal samples, the wetting process occurs rapidly. The heat release rate reaches its peak at 1.98 min. This is because in the initial wetting stage of the coal sample with water, a large amount of the coal sample surface is replaced by water, resulting in a decrease in surface free energy and much heat release. After reaching the peak heat release rate, water molecules continuously diffuse from the outer surface to the inner surface of the coal sample and cover the surface of the large and medium pores of the coal dust. Due to the influence of pore resistance, the wetting rate decreases and the wetting heat release rate declines. After 15 min, water molecules begin to wet the micropores inside the coal dust, entering a slow wetting stage and gradually reaching wetting equilibrium. At this stage, due to the capillary phenomenon, water molecules continuously penetrate into the voids inside the coal dust that are not occupied by water molecules, releasing a small amount of heat.

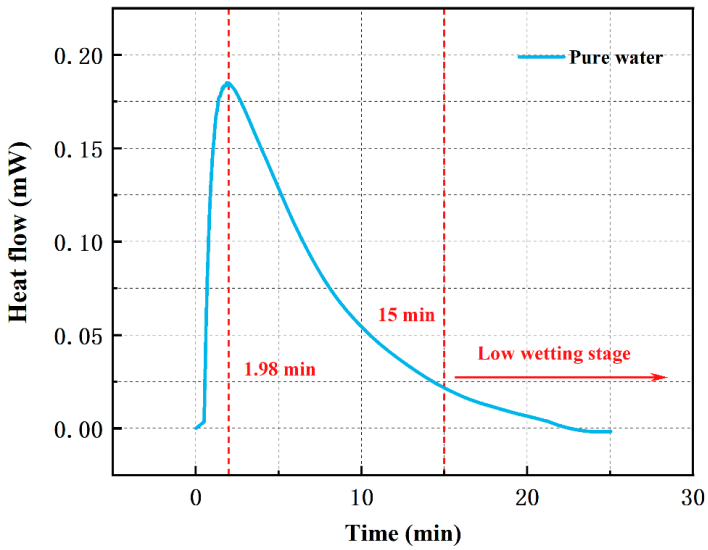


Figure 9. Wetting heat flow curves of pure water moistening coal sample.

3.4.2. Peak Time of Wetting Heat Flow Curves

Because the wetting heat value is very small, surfactant solutions at concentrations of 0.005% and 0.1% were selected to make the comparison more obvious. Figure 10 shows the wetting heat flow curves of the three surfactants at the two concentrations. Similarly to pure water, the wetting heat of the three surfactants increases rapidly in the initial stage.

Then, the wetting heat release rate gradually declines. Finally, the wetting process enters the slow wetting stage and gradually reaches wetting equilibrium.

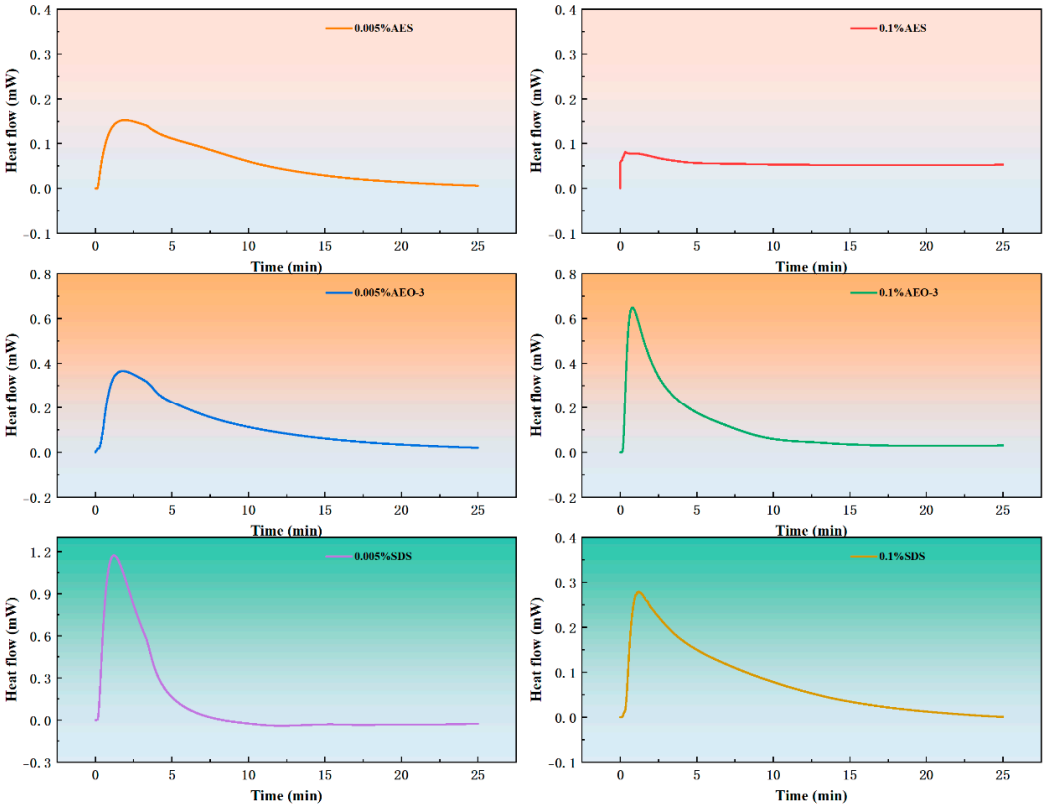


Figure 10. Wetting heat flow curves of surfactants at different concentrations.

Table 5 shows the peak time of the three surfactants' wetting heat flow curves. It can be seen that the time for the three surfactants wetting heat flow curves to reach the peak value decreases with the increase in surfactant concentration. This is because as the surfactant concentration increases, the surface tension of the surfactant solution declines, and the energy barrier for coal dust to enter the solution decreases. At the same time, the number of free surfactant molecules in the solution increases, and the number of surfactant molecules in contact with the coal dust hydrophobic sites is higher than that at low concentrations. Therefore, the interaction between surfactant molecules and coal dust is enhanced, quickly covering the surface of coal dust, resulting in a shorter peak time of the heat flow curves.

Table 5. Peak time of three surfactants' wetting heat flow curves.

Surfactant	Peak Time (min)		
	0%	0.005%	0.1%
SDS	1.98	1.22	1.21
AES	1.98	1.94	0.34
AEO-3	1.98	1.80	0.80

It can also be found that the peak time of the three surfactants at the concentration of 0.1% presents AES < AEO-3 < SDS, which is opposite to the order of adsorption density in Section 3.3. This indicates that the peak time of surfactants' wetting heat flow curves are related to the difference in surfactant adsorption state on the coal dust surface. The specific reasons are as follows. As shown in Figure 8b, the AES molecules form a bilayer adsorption structure, with its outer layer exhibiting surfactant hydrophobic groups facing outward.

As a result, the exothermic sites of AES molecules on the coal dust surface are reduced, and the surfactant solution can cover the hydrophilic water points on the outer surface of coal dust more quickly. This results in the shortest peak time of the wetting heat flow curves. For SDS, the SO_4^{2-} groups are negatively charged and have high electrostatic repulsion with each other. This creates resistance to the surfactant molecules replacing the coal dust surface. Thus, the adsorption process of SDS is the most difficult, leading to the longest peak time of the wetting heat flow curves. The nonionic surfactant AEO-3 is uncharged and has no electrostatic force. At the same time, it contains the EO groups with a certain degree of hydrophilicity, thus resulting in the second highest adsorption density and the peak time of the wetting heat flow curves.

3.4.3. Wetting Heat Value

The surface of coal dust contains a large number of hydrophobic sites, mainly composed of hydrocarbon chains and aromatic rings, which is the reason for the strong hydrophobicity of coal dust. A small number of oxygen-containing functional groups constitute the hydrophilic sites and are negatively charged. There is a strong hydrophobic interaction between the hydrocarbon chains and aromatic rings in coal dust and the tail chains of surfactants. This causes the surfactant hydrophobic groups adsorbed on the surface of the coal dust to face toward the coal dust and the hydrophilic end to back away from the coal dust surface and this can convert the hydrophobic sites of coal dust into hydrophilic sites and enhance the hydrophilicity of coal dust. At this time, the coal dust containing more hydrophilic sites is wetted with water, i.e., a larger heat value of wetting is generated. The wetting heat value per unit mass of coal sample is obtained by integrating the heat flow curve. The first 25 min of the wetting heat flow curves are selected, and the integration results (wetting heat value) of the wetting heat flow curves are listed in Table 6. The order is AEO-3 > SDS > AES. The reason is explained as follows.

Table 6. Wetting heat values for the three surfactants.

Surfactant	Wetting Heat Value (J/g)		
	0%	0.005%	0.1%
SDS	1.38	2.92	1.92
AES	1.38	1.41	1.40
AEO-3	1.38	2.96	2.78

Firstly, SDS is an anionic surfactant. Observing Figure 8a, it can be found that there is electrostatic repulsion between SDS surfactant molecules in the adsorbed monolayer. The negative charge carried by the SO_4^{2-} groups in the adsorbed SDS molecules will hinder adjacent SDS surfactant molecules from adsorbing onto the coal dust surface. Therefore, the adsorption density of SDS molecules adsorbed on the coal dust surface ranks the second, as does the number of hydrophilic sites on the coal dust surface, which results in the second wetting heat value among the three surfactants.

Secondly, as shown in Figure 8b, the EO groups in AES molecules attract some Na^+ ions to distribute around them. This results in some AES molecules that appear negatively charged after ionization binding with Na^+ ions. Due to the bilayer adsorption structure, some hydrophobic sites on the coal dust surface that should have been converted into hydrophilic sites still exhibit hydrophobicity. Therefore, the AES surfactant has the lowest wetting calorific value on coal samples, which is consistent with the results of wetting time.

Finally, as shown in Figure 8c, there is no electrostatic repulsion between AEO-3 surfactant molecules. Meanwhile, AEO-3 molecules do not form a bilayer adsorption structure on the coal dust surface. Thus, the adsorption density of the AEO-3 surfactant is

higher than that of SDS. This means that AEO-3 has the most hydrophilic water points on the coal dust surface. In addition, the EO groups in the AEO-3 surfactant molecules can enhance the wetting degree between coal dust and water. Supported by these two reasons, the AEO-3 surfactant produces the highest wetting heat value.

The rank of the wetting heat values by the three surfactants is consistent with the order of surface tension and wetting time. This indicates that in the wettability experiment of three surfactants on the coal dust, the nonionic surfactant AEO-3 containing EO groups is superior to the anionic surfactant SDS containing SO_4^{2-} groups and the anionic–nonionic surfactant AES containing both EO and SO_4^{2-} groups.

4. Conclusions

Surfactants with different hydrophilic group structures have different adsorption states and wetting effects on coal dust. In this work, three surfactants with similar hydrophilic groups, i.e., SDS, AES, and AEO-3, were specially chosen. Through surface tension, wetting time, infrared spectra, and wetting heat experiments, the effect of hydrophilic group structures of different surfactants on their adsorption states and wetting mechanism on coal dust was analyzed. This resulted in the following findings:

(1) With the increase in surfactant concentration, the surface tension decreased first and then stabilized, while the wetting time continued to decrease, which proved that surface tension was not the only factor affecting the wetting effect. The wetting ability of nonionic surfactant AEO-3 was completely superior to anionic surfactant SDS and anionic-nonionic surfactant AES. But, the FTIR results showed that AES and SDS had the highest and lowest adsorption density, respectively. In the wetting heat experiment, there was a negative correlation between the peak time of the wetting heat curves and the adsorption density, and a positive correlation between the wetting heat value and the wetting ability of the surfactant. Therefore, the different adsorption states on the coal dust surface caused by different hydrophilic group structures of surfactants would also affect the wetting effect significantly.

(2) The EO groups in the AES surfactant molecules could adsorb some free positively charged Na^+ ions in the solution around it. This led to the combination of EO groups with Na^+ ions, forming the bilayer adsorption structure and resulting in the highest adsorption density. However, the bilayer adsorption structure also caused the hydrophobic groups of AES molecules in the outer layer to face outward. This resulted in incomplete conversion of hydrophobic sites on the coal dust surface into hydrophilic sites. Therefore, AES had the weakest wetting ability and the lowest wetting heat.

(3) For SDS and AEO-3 surfactants, a monolayer adsorption structure was formed. The hydrophilic groups of surfactants faced outward, making the hydrophobic sites on the coal dust surface transform into hydrophilic sites. Thus, the wetting ability of SDS and AEO-3 was better than that of AES. Due to the electrostatic repulsion between adjacent SDS molecules, the intermolecular distance increased, resulting in the lowest adsorption density. Owing to the absence of electrostatic repulsion and the presence of EO groups, AEO-3 had higher adsorption density than SDS, resulting in the best wetting performance and highest wetting heat.

Author Contributions: Conceptualization, C.X., T.Z., S.W. and H.W.; methodology, C.X.; investigation, T.Z.; resources, C.X., S.W., J.G. and H.W.; writing—original draft preparation, T.Z.; writing—review and editing, S.W. and J.G.; funding acquisition, C.X. and H.W. All authors have read and agreed to the published version of the manuscript.

Funding: This research was funded by the National Natural Science Foundation of China (52104212 and 52322404), the National Key R&D Program of China (2023YFC3008804), the Key Research and Development Project of Hubei Province (2023DJC166), the Anhui Provincial Natural Science Foundation (2408085ME148), and the Fundamental Research Funds for the Central Universities.

Data Availability Statement: The original contributions presented in this study are included in the article. Further inquiries can be directed to the corresponding author.

Conflicts of Interest: The authors declare no conflicts of interest.

References

1. BP. *BP Statistical Review of World Energy 2023*; The United Kingdom of Great Britain and Northern Ireland: London, UK, 2023.
2. Li, Z.L.; Li, H.; Li, W.H.; Sun, J.P.; Li, K.Y. Organic Geochemical Features of the Upper Paleozoic Coal-Bearing Deposits in Ordos Basin, North-Central China. *Energies* **2023**, *16*, 15. [CrossRef]
3. Zhou, S.; Tong, Q.; Pan, X.Z.; Cao, M.; Wang, H.L.; Gao, J.; Ou, X.M. Research on low-carbon energy transformation of China necessary to achieve the Paris agreement goals: A global perspective. *Energy Econ.* **2021**, *95*, 11. [CrossRef]
4. Wu, Y.; Meng, X.; Zhang, Y.; Shi, L.; Wu, Q.; Liu, L.; Wang, Z.; Liu, J.; Yan, K.; Wang, T. Experimental study on the suppression of coal dust explosion by silica aerogel. *Energy* **2023**, *267*, 126372. [CrossRef]
5. Cao, W.; Qin, Q.; Cao, W.; Lan, Y.; Chen, T.; Xu, S.; Cao, X. Experimental and numerical studies on the explosion severities of coal dust/air mixtures in a 20-L spherical vessel. *Powder Technol.* **2017**, *310*, 17–23. [CrossRef]
6. Yan, H.; Nie, B.; Peng, C.; Liu, P.; Wang, X.; Yin, F.; Gong, J.; Wei, Y.; Lin, S.; Gao, Q. Evaluation on explosion characteristics and parameters of pulverized coal for low-quality coal: Experimental study and analysis. *Environ. Sci. Pollut. Res.* **2022**, *29*, 18851–18867. [CrossRef]
7. Liang, G.Q.; Dai, H.M.; Yin, H.P.; Zhao, Q.; Chen, X.F. Inhibition characteristics of coal dust explosion at the gasification atmosphere. *Adv. Powder Technol.* **2021**, *32*, 3725–3734. [CrossRef]
8. Liu, Z.Q.; Zhou, G.; Li, S.L.; Wang, C.M.; Liu, R.L.; Jiang, W.J. Molecular dynamics simulation and experimental characterization of anionic surfactant: Influence on wettability of low-rank coal. *Fuel* **2020**, *279*, 118323. [CrossRef]
9. Guo, Q.; Ren, W.X.; Shi, J.T. Foam for coal dust suppression during underground coal mine tunneling. *Tunn. Undergr. Space Technol.* **2019**, *89*, 170–178. [CrossRef]
10. Han, F.W.; Peng, Y.Y.; Zhao, Y.; Yang, P.; Hu, F.H. Comparative investigation of methods for evaluating the wettability of dust suppression reagents on coal dust. *J. Mol. Liq.* **2024**, *399*, 124380. [CrossRef]
11. Zhang, T.; Jing, D.J.; Ge, S.C.; Wang, J.R.; Chen, X. Supersonic antigravity aerodynamic atomization dusting nozzle based on the Laval nozzle and probe jet. *J. Braz. Soc. Mech. Sci. Eng.* **2020**, *42*, 335. [CrossRef]
12. Yuan, M.Y.; Nie, W.; Zhou, W.W.; Yan, J.Y.; Bao, Q.; Guo, C.J.; Tong, P.; Zhang, H.H.; Guo, L.D. Determining the effect of the non-ionic surfactant AEO9 on lignite adsorption and wetting via molecular dynamics (MD) simulation and experiment comparisons. *Fuel* **2020**, *278*, 118339. [CrossRef]
13. Xu, C.H.; Lin, Z.K.; Zhou, G.; Hu, X.M.; Wang, H.T.; Chen, X.F. Effect of welan gum and carbomer on foam and wetting properties of sodium alpha-olefin sulfonate for coal dust control. *J. Mol. Liq.* **2023**, *388*, 122692. [CrossRef]
14. Gan, J.; Wang, D.M.; Xiao, Z.M.; Wang, Y.N.; Zhang, K.; Zhu, X.L.; Li, S.L. Experimental and molecular dynamics investigations of the effects of ionic surfactants on the wettability of low-rank coal. *Energy* **2023**, *271*, 127012. [CrossRef]
15. Han, F.W.; Hu, F.H.; Zhao, X.L.; Liu, M.; Yang, P.; Niu, G.R. Study on the effect of electrolyte on surface tension of surfactant solution and wettability of coal dust. *Colloid Surf. A-Physicochem. Eng. Asp.* **2024**, *682*, 132929. [CrossRef]
16. Han, F.W.; Liu, M.; Hu, F.H.; Zhao, Y.; Peng, Y.Y. Spreading Behavior and Wetting Characteristics of Anionic Surfactant Droplets Impacting Bituminous Coal. *ACS Omega* **2022**, *7*, 46241–46249. [CrossRef]
17. Li, J.J.; Yan, G.C.; Kong, S.Q.; Bai, X.Y.; Li, G.; Zhang, J.W. Molecular Mechanism Study on the Effect of Microstructural Differences of Octylphenol Polyoxyethylene Ether (OPEO) Surfactants on the Wettability of Anthracite. *Molecules* **2023**, *28*, 4748. [CrossRef]
18. Zhou, Q.; Qin, B.T. Coal dust suppression based on water mediums: A review of technologies and influencing factors. *Fuel* **2021**, *302*, 121196. [CrossRef]
19. Marinova, K.G.; Naydenova, K.T.; Basheva, E.S.; Bauer, F.; Tropsch, J.; Franke, J. New surfactant mixtures for fine foams with slowed drainage. *Colloid Surf. A-Physicochem. Eng. Asp.* **2017**, *523*, 54–61. [CrossRef]
20. Chang, P.; Xu, G.; Chen, Y.P.; Ghosh, A.; Moridi, M.A. Improving coal powder wettability using electrolyte assisted surfactant solution. *Colloid Surf. A-Physicochem. Eng. Asp.* **2021**, *613*, 126042. [CrossRef]
21. Wang, Q.G.; Wang, D.M.; Wang, H.T.; Xu, C.H. Influence of alkyl polyglucoside and fatty alcohol ether sulfate on the foaming and wetting properties of sodium dodecyl benzene sulfonate for mine dust control. *Powder Technol.* **2019**, *345*, 91–98. [CrossRef]
22. Liu, Z.; Jiao, L.S.; Yang, H.; Zhu, M.Y.; Zhang, M.M.; Dong, B.W. Study on the microstructural characteristics of coal and the mechanism of wettability of surfactant solutions at different pH levels. *Fuel* **2023**, *353*, 129268. [CrossRef]

23. Chen, M.; Lu, X.C.; Liu, X.D.; Hou, Q.F.; Zhu, Y.Y.; Zhou, H.Q. Specific Counterion Effects on the Atomistic Structure and Capillary-Waves Fluctuation of the Water/Vapor Interface Covered by Sodium Dodecyl Sulfate. *J. Phys. Chem. C* **2014**, *118*, 19205–19213. [CrossRef]
24. Xu, C.H.; Mandal, T.; Larson, R.G.; Wang, D.M.; Wang, H.T. A molecular dynamics simulation of the structure of sodium lauryl ether sulfate and poly(vinyl alcohol) at the air/water interface. *Colloid Surf. A-Physicochem. Eng. Asp.* **2019**, *563*, 84–94. [CrossRef]
25. Crawford, R.J.; Mainwaring, D.E. The influence of surfactant adsorption on the surface characterisation of Australian coals. *Fuel* **2001**, *80*, 313–320. [CrossRef]
26. Xu, C.H.; Wang, D.M.; Wang, H.T.; Ma, L.Y.; Zhu, X.L.; Zhu, Y.F.; Zhang, Y.; Liu, F.M. Experimental investigation of coal dust wetting ability of anionic surfactants with different structures. *Process Saf. Environ. Protect.* **2019**, *121*, 69–76. [CrossRef]
27. Liu, S.Y.; Liu, X.Y.; Guo, Z.Y.; Liu, Y.T.; Guo, J.Y.; Zhang, S.H. Wettability modification and restraint of moisture re-adsorption of lignite using cationic gemini surfactant. *Colloid Surf. A-Physicochem. Eng. Asp.* **2016**, *508*, 286–293. [CrossRef]
28. Wang, X.N.; Yuan, S.J.; Jiang, B.Y. Experimental investigation of the wetting ability of surfactants to coals dust based on physical chemistry characteristics of the different coal samples. *Adv. Powder Technol.* **2019**, *30*, 1696–1708. [CrossRef]
29. Tessum, M.W.; Raynor, P.C.; Keating-Klika, L. Factors Influencing the Airborne Capture of Respirable Charged Particles by Surfactants in Water Sprays. *J. Occup. Environ. Hyg.* **2014**, *11*, 571–582. [CrossRef]
30. Xu, H.; Penfold, J.; Thomas, R.K.; Petkov, J.T.; Tucker, I.; Webster, J.P.R. The Formation of Surface Multi layers at the Air-Water Interface from Sodium Polyethylene Glycol Monoalkyl Ether Sulfate/$AlCl_3$ Solutions: The Role of the Size of the Polyethylene Oxide Group. *Langmuir* **2013**, *29*, 11656–11666. [CrossRef]
31. Jang, S.S.; Goddard, W.A., III. Structures and properties of newton black films characterized using molecular dynamics simulations. *J. Phys. Chem. B* **2006**, *110*, 7992–8001. [CrossRef]
32. Hao, B.; Fan, M.Q.; Li, H.P. Adsorption process and mechanisms of AEO-3/dodecane mixed collector on low-rank coal surface driven by water flow: A non-equilibrium molecular dynamics simulation study. *J. Mol. Liq.* **2022**, *364*, 119993. [CrossRef]
33. Zheng, R.J.; Ren, Z.J.; Gao, H.M.; Qian, Y.P. Evaluation of Sulfonate-Based Collectors with Different Hydrophobic Tails for Flotation of Fluorite. *Minerals* **2018**, *8*, 57. [CrossRef]
34. Bera, A.; Kumar, T.; Ojha, K.; Mandal, A. Adsorption of surfactants on sand surface in enhanced oil recovery: Isotherms, kinetics and thermodynamic studies. *Appl. Surf. Sci.* **2013**, *284*, 87–99. [CrossRef]
35. Pucic, I.; Jurkin, T. FTIR assessment of poly(ethylene oxide) irradiated in solid state, melt and aqueous solution. *Radiat. Phys. Chem.* **2012**, *81*, 1426–1429. [CrossRef]
36. Zhanzakova, A.; Tong, S.Y.; Yang, K.J.; Chen, L.; Li, K.J.; Fu, H.B.; Wang, L.; Kong, L.D. The effects of surfactants on the heterogeneous uptake of sulfur dioxide on hematite. *Atmos. Environ.* **2019**, *213*, 548–557. [CrossRef]
37. Du, C.T.; Kong, L.D.; Zhanzakova, A.; Tong, S.Y.; Yang, X.; Wang, L.; Fu, H.B.; Cheng, T.T.; Chen, J.M.; Zhang, S.C. Impact of adsorbed nitrate on the heterogeneous conversion of SO_2 on α-Fe_2O_3 in the absence and presence of simulated solar irradiation. *Sci. Total Environ.* **2019**, *649*, 1393–1402. [CrossRef]
38. Smith, B.C. Group Wavenumbers and an Introduction to the Spectroscopy of Benzene Rings. *Spectroscopy* **2016**, *31*, 34–37.
39. Al-Sabagh, A.M.; Azzam, E.M.S.; Mahmoud, S.A.; Saleh, N.E.A. Synthesis of ethoxylated alkyl sulfosuccinate surfactants and the investigation of mixed solutions. *J. Surfactants Deterg.* **2007**, *10*, 3–8. [CrossRef]
40. Xu, C.H.; Wang, H.T.; Wang, D.M.; Zhu, Y.F.; Zhu, X.L.; Yu, H. Study on the mechanism of polyethylene oxide groups improving the foamability of anionic surfactants in hard water. *Colloid Surf. A-Physicochem. Eng. Asp.* **2021**, *613*, 126046. [CrossRef]
41. Allardice, D.; Evans, D. The-brown coal/water system: Part 2. Water sorption isotherms on bed-moist Yallourn brown coal. *Fuel* **1971**, *50*, 236–253. [CrossRef]

Disclaimer/Publisher's Note: The statements, opinions and data contained in all publications are solely those of the individual author(s) and contributor(s) and not of MDPI and/or the editor(s). MDPI and/or the editor(s) disclaim responsibility for any injury to people or property resulting from any ideas, methods, instructions or products referred to in the content.